2023-10

A climate perturbation at the Middle Late Jurassic Transition? Evaluating the isotopic evidence from south-central England

Watanabe, Sayaka

10.1016/j.palaeo.2023.111755
Palaeogeography, Palaeoclimatology, Palaeoecology
Elsevier BV

A climate perturbation at the Middle –Late Jurassic Transition? Evaluating the isotopic evidence.

Gregory D. Price*[1], Bernát Heszler[1,2], Lauren-Marie Tansley Charlton[1], Jade Cox[1]

[1]School of Geography, Earth and Environmental Sciences

University of Plymouth, Plymouth, UK, PL4 8AA

[2] Department of Geology, Eötvös Loránd University, Pázmány Péter sétány 1/C,

Budapest H-1117, Hungary

*Corresponding author

Abstract The Jurassic greenhouse is punctuated by short cooling intervals with at times postulated polar ice-sheet development. Published oxygen isotope records of belemnite rostra and fish teeth have been interpreted to reveal a prominent decrease in seawater temperature during the Late Callovian–Early Oxfordian. This is in part the basis for a proposed an ice age at the Middle-Late Jurassic Transition. In contrast relatively constant oxygen isotope records and therefore seawater temperatures and carbon isotope values characterized by significant scatter but showing more positive values during the middle and late Callovian have been reported from elsewhere. This research has constructed a stable isotope stratigraphy (from belemnites, Gryphaea and oysters) principally from the Callovian-Oxfordian interval (from southern England) and integrated these data with existing data to assess the pattern of carbon and oxygen isotopic change. Our marine macrofossil record reveals isotopic patterns that are generally comparable with other European basins. Carbon isotopic trends are consistent with bulk carbonate carbon isotope records displaying systematic fluctuations, the largest of which (Middle Callovian, Calloviense/Jason Zones to Early Oxfordian, Mariae Zone) corresponds to previously identified phases of environmental perturbation. Such a trend may have resulted from enhanced burial and preservation of organic matter, leaving the seawater more positive in terms of carbon. Inferred cooling, derived from our oxygen isotope data from southern England, occurs within the Late Callovian and Oxfordian (Athleta to Mariae zones). Cooling post-dates this positive carbon isotope excursion. Enhanced carbon burial and atmospheric carbon dioxide draw down may have induced cooling. In this study the analysis of a single region (southern England) allows some constraints on potential variables that may influence isotope records. If Jurassic polar climates were truly warm such a degree of cooling would undoubtedly lead to cooler polar temperatures – but only with seasonal ice.

Key words: Dorset; Jurassic; Callovian; Oxfordian; carbon and oxygen isotopes; belemnites, Gryphaea; oysters

1. Introduction

The Jurassic greenhouse is punctuated by short cooling intervals with at times postulated polar ice-sheet development (Dromart et al., 2003; Dera et al., 2011; Donnadieu et al. 2011; Nordt, et al., 2021). These cold intervals have been classically attributed to a transient atmospheric CO_2 drawdown. For example, late Pliensbachian and early Toarcian expanding polar ice caps, global cooling and sea level variations have been linked to carbon cycle changes (Krenker et al. 2019; Ruebsam and Al-Husseini 2021). Likewise, cooling and a proposed an ice age at the Middle-Late Jurassic (Late Callovian–Early Oxfordian) transition has been linked to reduced CO_2 (Dromart et al., 2003) and evidenced through oxygen isotope records of belemnite rostra and fish teeth from the Russian Platform, eastern France and western Switzerland (e.g., Barskov and Kiyashko, 2000; Dromart et al., 2003; Lécuyer et al., 2003). In contrast relatively constant oxygen isotope records and therefore seawater temperatures and $\delta^{13}C$ values characterized by significant scatter but showing more positive values during the middle and late Callovian have been reported from central Poland, Russia and India (Wierzbowski et al., 2009; Alberti et al., 2012). Global cooling and the presence of major continental ice caps during the Jurassic continues to be the subject of debate (e.g., Korte and Hesselbo, 2011; Wierzbowski and Rogov, 2011; Krencker et al., 2019; Ruebsam and Al-Husseini 2021). The aim of this research is to describe and evaluate a stable isotope stratigraphy from the Callovian-Oxfordian interval and integrate these data with existing isotopic records to assess the pattern of carbon and oxygen isotopic changes. Through analysis of a single region (southern England) allows some constraints on potential variables that may influence isotope records to be fully assessed.

2. Geological Setting and Sampling Locations

During the Middle to Late Jurassic Europe was flooded by a shallow epeiric sea (Fig. 1). Britain's palaeolatitude (40°N), placed it directly between the carbonate platform of the Tethys Ocean, the proto-Atlantic and the Boreal Sea siliciclastic dominated sequences with faunas being typically intermediate between the two (Price and Page, 2008; Wierzbowski et al., 2013; Pellenard et al., 2014; Cope, 2016). Southern England consisted of partly emergent land masses, namely the London-Brabant Massif to the east, the Armorican Massif to the south and the smaller Cornubian and Welsh Massif's to the west. As detailed below, belemnite, oyster and Gryphaea samples were collected from multiple locations across Dorset, Wiltshire and Cambridgeshire, UK (Figs 1-3).

2.1 Burton Cliff, Burton Bradstock, Inferior Oolite

The oldest samples examined is this study come from the Bajocian Inferior Oolite at Burton Cliff, Burton Bradstock, Dorset, UK (Fig. 2). These are bioturbated and fossiliferous limestones (Callomon and Cope, 1995; Cope, 2016). Samples were collected from the Snuff-boxes, the Red Conglomerate Bed and Beds 13 and 14. The Snuff-boxes horizon is marly, blue grey oolitic limestone, with ellipsoidal, laminated oncolytic biscuits ('snuff-boxes') (Palmer and Wilson 1990; Callomon and Cope, 1995). Ammonites previously identified represent the Discites Zone. The Red Conglomerate bed comprises of ironshot, chamositic oolites, spanning the Humphriesianum and Subfuracatum Zones (Callomon and Cope, 1995). Bed 13 (the Truellei Bed) is marly limestone and with scattered ooids and contains ammonites from the Parkinsoni Zone, Truelli Subzone (Callomon and Cope, 1995). Bed 14 is a limestone with echinoderms, large nautiloids, brachiopods, sponges and bivalves. Ammonites include *Parkinsonia bombfordi* (Parkinsoni zone, bombfordi Subzone) (Callomon and Cope, 1995).

2.2 Kellaways, River Avon, Kellaways Sand Member

Callovian samples were derived from the type locality of the Kellaways Formation (Page, 1989), located on the river Avon, west of Tytherton, Wiltshire, UK. Although the exposure is limited (Fig. 2), the basal Kellaways Clay Member is overlain by the Kellaways Sand Member, consisting of bioturbated silts and calcareous sands (Page, 1989; Hudson and Martill, 1991). Fossils include ammonite's representative of the Calloviense Subzone, belemnites (*Cylindroteuthis*) and benthic bivalves (Page, 1989; Hudson and Martill, 1991).

2.3 Yaxley Clay Pit, Cambridgeshire, Peterborough Member

At Yaxley, Cambridgeshire, the Peterborough Member (Jason Zone) of the Oxford Clay formation is exposed in a former clay pit (Hudson and Martill, 1991) and contains crushed aragonitic ammonites, belemnites and gryphaea. Belemnites (*H. Hastata*) and Gryphaea (*G. dilobote*s) samples were obtained from Yaxley.

2.4 Fleet Lagoon, Dorset, Oxford Clay

Belemnite, oyster and Gryphaea samples were obtained from exposures at Tidmoor Point and Furzedown, Fleet Lagoon, Dorset. At Tidmoor Point the Oxford Clay, Lamberti Zone (Callomon and Cope 1995) comprises of bioturbated calcareous clays and includes *Kosmeroceras* and *Quenstedtoceras* and other abundant fossils including the large *Gryphaea lituola* and belemnites (including *H. hastata)* (Callomon and Cope, 1995; Cope, 2016). Belemnite (*H. hastata*) and Gryphaea (*G. lituola*) samples were also obtained from the Furzedown Clay Member (Mariae Zone, Scarburgense subzone, Wright, 1986), Oxford Clay at Furzedown of the Dorset, Fleet (Arkell 1947).

2.5 Redcliff Point, Dorset, Oxford Clay

Belemnite and Gryphaea samples were obtained from Redcliff Point near Weymouth, Dorset (Fig. 2), where a Callovian-Oxfordian boundary succession is exposed (Arkell, 1947; Wright, 1986). The section has consequently been proposed as a candidate GSSP for the base of the latter stage. The samples were obtained from the Weymouth Member (Lamberti and Scarburgense Zones and subzones). The Weymouth member consist of a relatively hard medium to pale grey claystones and marls and were deposited in waters reaching a few tens of metres in depth (Hudson and Martill, 1991). The succession also contains the belemnite *H. hastata,* generally uncommon oxytomid bivalves and *G.* ex grp *dilatata*. Of these, belemnites (*H. hastata*); and Gryphaea (*G.* ex grp *dilatata*) were analysed.

2.6 Sandridge Park, Wiltshire, Sandridge Member

The principal exposure, type locality and sampling location of the Sandridge Member, is at the Sahara Sand Quarry (Sandridge Pit, Melksham Quarry, Wiltshire), comprising of a cross-bedded shelly and bioturbated shelly sands (Wright, 2014). This large sand pit is now a landfill site, with limited exposure. Bed 2 is the only remaining unit left exposed, a tempestite deposit, consisting of coarse-grained bioturbated shelly sands (Wright, 2014). The fossils derived from this location include *Liostrea*. The Sandridge Member belongs to the Cordatum Zone (Cordatum Subzone, Wright, 2014).

2.7 Sandsfoot Castle, Weymouth, Sandsfoot Grit Member

Belemnite and oyster (*Deltoideum delta*) samples were collected from the Sandsfoot Grit Member (Pseudocordata Zone (Regulare-Rosenkrantzi), Pseudoyo subzone, Wright 1986) from cliffs exposed beneath Sandsfoot Castle, Dorset (Fig. 2). Here the sediments consist of bioturbated sandy ironstones with chamosite ooids suggesting shallow, high energy deposition (Cope, 2016).

3. **Methodology**

Optical microscopy and cathodoluminescence (CL) analysis, in conjunction with elemental geochemistry, was undertaken in order to determine the state of preservation of each fossil specimen examined. Polished thin sections were prepared from representative specimens collected from each locality. CL was undertaken using a CITL Mk5-2 luminescence model, coupled with a Nikon Eclipse 50iPOL microscope. For elemental geochemistry and stable isotopes, calcite fragments judged to be best preserved were selected. The criteria being transparent honey coloured calcite, avoiding any dark brown or frosted fragments. Weighed calcites were dissolved in nitric acid and elemental concentrations (Ca, Mg, Sr, Mn and Fe) were generated using a Thermo Scientific iCAP 7000 Plus Inductively Coupled Plasma Optical Emission Spectrometer (ICP-OES) at the University of Plymouth. The reference material JLs-1 Limestone was also included in the ICP-OES analysis. Stable isotope data were generated on a Thermo Scientific Delta V Advantage with a Gasbench II online gas preparation module at the Stable Isotope Laboratory, University of Plymouth. Isotope ratios were calibrated using NBS-19 standard and are given in δ notation relative to the Vienna Pee Dee Belemnite (VPDB). Reproducibility was typically better than 0.1‰ for all samples and standard materials.

4. **Results**

4.1 Petrographic and CL analysis

The belemnites were typically honey coloured typical of pristine primary calcite. Most of the diagenetic alteration observed occurred around the outer margins (Fig. 4) and in the apical regions revealing sparry calcite re-crystallisation (consistent with other studies, e.g., Price and Teece, 2010; Wierzbowski and Rogov, 2011; Mettam et al., 2014). Using CL, the belemnite rostra examined were in general non-luminescent. The main areas of luminescence were the outer shell margins and the apical regions and along any prominent cracks/microfractures.

Petrographic and CL analysis of the oyster specimens showed mostly non-luminescent, well-preserved foliated shells, representing primary calcite. The main areas of alteration identified were along the outer shell rims, along prominent fractures, within borings and within interspersed lens shaped chambers. These chambers are seen interspersed throughout the shell and were possibly previously occupied with porous chalky calcite (e.g., Banker and Sumner, 2020). For example, the samples from Tidmoor Point, and Sandsfoot Castle, show luminescent sparry calcite and infilled microborings along the outer margins, and cross cutting veins and spar in spaces within the shells. These areas (Fig. 5) were avoided during subsampling for stable isotopes. The Gryphaea samples were characterised by typical pristine branching cross foliation structures (e.g., Malchus and Aberhan, 1998) (Fig. 5) and were largely non-luminescent. Some evidence of diagenetic alteration was observed, with sparry calcite present on the shell margins. Some showed fractures infilled with matrix and luminescent sparry calcite re-crystallisation (Fig. 5).

4.2 Elemental Geochemistry

Element concentrations (Fe, Mn, Mg, Sr, and Ca) were obtained to assess the degree of diagenetic alteration (Appendix 1). Fe and Mn concentrations are typically higher in diagenetically altered calcite, as Fe^{2+} and Mn^{2+} are more soluble under reducing conditions and thus available for replacing Ca^{2+} in the calcite lattice (Brand and Veizer 1980). Increases in Mn and Fe are often mirrored by decreases in Mg and Sr. Bivalves (including oysters and Gryphaea) typically show more variable in Fe and Mn concentrations compared to belemnites (Anderson et al., 1994; Price and Page, 2008; Price and Teece, 2010). For belemnites, the Mg concentrations ranged between 903 and 5292 ppm (mean 2371 ppm), for Sr between 660 and 1819 (mean 1013 ppm) and 25.6 and 59.3% (mean 40.0%) for Ca. The total determined Mn and Fe values ranged between 2 and 548 ppm (mean 36ppm) for Mn, and between 30 and 1115 ppm (mean 190 ppm, excluding the single very high value) for Fe (Appendix). Belemnite specimens with high concentrations of Mn (>150ppm) and Fe (>300 ppm) were determined to be possibly diagenetically altered (cf. Price and Teece, 2010; Wierbowski 2004; Ditchfield 1997) and were excluded from further analysis.

For the oysters and Gryphaea, the Mg concentrations ranged between 273 and 1249 ppm (mean 444 ppm), Sr between 401 and 807 (mean 574 ppm) and 24.0 and 52.8% (mean 41.0%) for Ca. Determined Mn and Fe values ranged between 6 and 207 ppm (mean 59 ppm) for Mn, and between 30 and 1115 ppm (mean 318 ppm) for Fe (Appendix). Bivalves (including Gryphaea and oysters) are typically characterized by quite variable Fe and Mn contents (e.g., Milliman, 1974; Anderson et al. 1994; Korte and Hesselbo, 2011; Price and Page 2008). The Gryphaea and oyster samples with high Fe and Mn concentration were excluded from further analysis. Overall, most belemnites, oysters and Gryphaea are deemed well preserved.

4.3 Oxygen isotopes

The well-preserved belemnite $\delta^{18}O$ values of this study display a modest variability, ranging between −2.1‰ and +0.7‰ (V-PDB) (averaging −0.5‰)(Fig. 6). These data have been combined with well-preserved belemnite calcite oxygen isotope data from Jenkyns et al. (2002); Price et al. (2009), Price and Page (2008), Price et al. (2015), Li et al. (2013), Anderson et al. (1994) and Price and Teece (2010) from the same region (see Figs. 1, 3). Stratigraphically, the $\delta^{18}O$ values show more positive values during the Bajocian, reaching +0.7‰ in the Parkinsoni zone (Truellei subzone)(Fig. 7). The $\delta^{18}O$ values then shift to more negative values during the Late Bajocian and the most negative values are seen within the Peterborough Member (Middle Callovian, Jason Zone). Subsequently the $\delta^{18}O$ values become more positive, reaching most positive values in the Late Callovian (Athleta Zone) and Early Oxfordian (Marie zone) (Fig. 7). A slight return to more negative

$\delta^{18}O$ values follows reaching the most negative (−1.3‰) in the Sandsfoot Grit Member (Oxfordian, Pseudocordata Zone, Pseudoyo Subzone).

The oyster and Gryphaea $\delta^{18}O$ values (Fig. 6) of this study display a larger variability ranging between −3.5‰ and +0.4‰ (V-PDB). The oyster and Gryphaea $\delta^{18}O$ values are slightly more negative on average compared to the belemnite $\delta^{18}O$ values (similar to the pattern seen by Price and Page, 2008; Mettam et al., 2014). These data have been combined with well-preserved belemnite calcite oxygen isotope data from Hendry and Kalin (1997), Price and Teece (2010), Price and Page (2008), Mettam et al. (2014), Anderson et al. (1994), Martin-Garin et al. (2010), Jenkyns et al. (2002) and Price et al. (2009). The stratigraphic $\delta^{18}O$ trends, are similar to the belemnite data, whereby $\delta^{18}O$ values show more positive values during the Bathonian, reaching +1.1‰ in the Retrocostatum zone. The $\delta^{18}O$ values then shift to more negative values with the most negative are seen within the Callovian (Calloviense Zone) at Kellaways and within Peterborough Member (Callovian, Jason Zone). Subsequently the $\delta^{18}O$ values become more positive, reaching most positive values in the Late Callovian (Lamberti Zone, Lamberti Subzone) at Redcliff Point (Fig. 8). A return to more negative $\delta^{18}O$ values follows reaching the most negative (−3.5‰) in the Sandsfoot Grit Member (Oxfordian, Pseudocordata Zone, Pseudoyo Subzone) and in the Kimmeridgian (the data of Jenkyns et al. 2002).

4.4 Carbon Isotopes

The belemnite $\delta^{13}C$ values of this study (Fig. 6) displayed a relatively large variability, ranging between −2.1‰ and +4.0‰ (V-PDB) (average +1.2‰). Combining with published data, stratigraphically the $\delta^{13}C$ values show positive values during the Bajocian and then shift to more negative values during the Bathonian (down to −2.3‰). Subsequently the $\delta^{13}C$ values become much more positive, reaching the most positive values in the Callovian (Calloviense−Jason Zones) at

Kellaways. Positive values are maintained until the early Oxfordian reaching a maximum of +3.6‰ at Redcliff Point (Mariae Zone, Scarburgense Subzone). A return to more negative $\delta^{13}C$ values follows reaching the most negative values (−0.5‰) in the Sandsfoot Grit Member (Oxfordian, Pseudocordata Zone, Pseudoyo Subzone).

The oyster and Gryphaea $\delta^{13}C$ values (Fig. 6) of this study display a larger variability ranging between +1.4‰ and +5.1‰ (V-PDB) (average +3.6‰). The oyster and Gryphaea $\delta^{13}C$ values are more positive compared to the belemnite $\delta^{13}C$ values. The Gryphaea show the most positive values (Fig. 6). These data have been combined with well-preserved oyster and Gryphaea calcite carbon isotope data from Price and Teece (2010), Price and Page (2008), Mettam et al. (2014), Anderson et al. (1994), Martin-Garin et al. (2010), Jenkyns et al. (2002) and Price et al. (2009). The stratigraphic $\delta^{13}C$ trends, are similar to the belemnite data, whereby $\delta^{13}C$ values show moderately positive values during the Bathonian, and then shift to more positive values within the Callovian (Calloviense Zone) at Kellaways. Within Peterborough Member (Callovian, Jason Zone) positive values are also seen although a considerable spread of values is observed. Positive carbon isotope values are seen also in the Furzedown Clay Member (Oxfordian, Mariae Zone) (reaching +4.9 ‰). A return to slightly less positive $\delta^{13}C$ values follows for the Sandridge Member (Oxfordian, Cordatum Zone) and the remainder of the Oxfordian through into the Kimmeridgian.

5. Discussion

Belemnite, oyster and Gryphaea $\delta^{13}C$ values have been found to be a reliable proxy for temporal changes of the isotope composition of the dissolved inorganic carbon (DIC) in ancient seas (Anderson et al., 1994; Price et al., 2000; Rosales et al., 2001; Wierzbowski, 2004; Wierzbowski and Joachimski, 2007; Price and Teece, 2010; Mettam et al., 2014). The observed scatter of coeval $\delta^{13}C$ values of belemnite rostra and oysters and Gryphaea shells may result from short-lived temporal changes in the isotope composition of the DIC in the ambient waters. Variations in biologic productivity as well as mixing of different DIC sources into the shallow middle and late Jurassic seas may account for some of these the temporal changes. The differences between the $\delta^{13}C$ values of belemnites, oysters and Gryphaea (Fig. 6) suggests that one or both groups may have been characterized by a different metabolic effect and/or differences linked to variation in ambient DIC associated with habitat. Nevertheless, both groups show comparable carbon trends through the examined interval.

A large positive carbon isotope shift seen in the middle Callovian (Calloviense-Jason Zones) and positive values are maintained until the early Oxfordian (Mariae Zone, Scarburgense Subzone). Such a trend may have resulted from enhanced burial and preservation of organic matter (e.g., Weissert, 1989), leaving the seawater more positive in terms of $\delta^{13}C$seawater. Dromart et al. (2003) for example identify Callovian organic-rich deposits including the Peterborough Member (Calloviense-Jason Zones) of the Oxford Clay Formation in England (Kenig et al., 1994), and the Tuwaiq Mountain Formation in Saudi Arabia (Carrigan et al., 1995). This positive excursion possibly represents a major carbon cycle perturbation recognized elsewhere in both oceanic and terrestrial reservoirs. Bartolini et al. (1999) and Katz et al. (2005) report a large positive carbon isotope excursion in the middle Callovian and remaining positive until the Middle Oxfordian from the Atlantic Ocean. A broad Callovian - Oxfordian peak is seen also in the organic carbon isotope record of Nunn et al. (2009) from Scotland. Other late Jurassic marine successions are also characterized by positive carbon isotope excursions occurring during the Middle Oxfordian (Jenkyns 1996; Wierzbowski, 2004; Louis-Schmid et al. 2007). Louis-Schmid et al. (2007) for example, locate peak carbon isotope values within the Plicatilis and Transversarium ammonite zones (see also Jenkyns, 1996). Pearce et al. (2005) also describe a mid-Oxfordian positive carbon-isotope excursion recognised from fossil wood principally from Scotland. Notably the studies of Louis-Schmid et al. (2007) and Jenkyns (1996) report little data from the Callovian – but when they do high positive ^{13}C values are also seen. In contrast, the belemnite isotope record of the Callovian–Oxfordian boundary in the Russian Platform, is described as being characterized by significant scatter and no temporal carbon isotope trend evident (Wierzbowski and Rogov, 2011).

Jurassic seawater paleotemperature reconstructions are frequently determined using the oxygen isotope composition of biogenic carbonate (e.g., Anderson et al. 1994; Dromart et al., 2003; Korte and Hesselbo, 2011). It is widely assumed that marine molluscs e.g., belemnites and oysters precipitate their rostra and shells in isotopic equilibrium with seawater (e.g., Anderson et al. 1994; Dromart et al., 2003; Price and Page, 2008; Nunn et al., 2009; Wierzbowski and Rogov, 2011; Pellenard et al., 2014). The equation of Anderson and Arthur (1983), and a δ value of −1‰ SMOW for an ice-free Earth, has typically been used. There is, however, much uncertainty regarding the −1‰ seawater value, for palaeotemperature reconstructions, because this value varies with changes in $\delta^{18}O_{seawater}$ (which can in turn be related to salinity) and ice-volume changes (Price and Teece, 2010; Pellenard et al. 2014). The modelling of Zhou et al., (2008) points to values at northern hemisphere temperate latitudes ranging from −1.0 and −2.0‰. A recent study looking at clumped isotopes and belemnites (Vickers et al. 2021) suggests that the equation of Kele et al. (2015), for slow-growing, abiotic calcites, when applied to well-preserved belemnite calcite, returns temperatures considerably warmer than the equation of Anderson and Arthur (1983) and δ^{18}Oseawater values within the expected range for open water to semi-enclosed basin setting (consistent with Zhou et al., 2008). That the $\delta^{18}O$ data from the belemnites, oysters and Gryphaea showing near similar tends through the examined interval suggests a consistency of the ambient waters affecting both the nektonic (belemnites) and benthic (oysters and Gryphaea) organisms. Evaluating the data presented here (Figs. 7, 8) and assuming a constant $\delta^{18}O_{seawater}$ value suggests a warm temperature shift of ~4 degrees from the Bajocian to Callovian (Peterborough Member, Jason Zone). Follows is a cooling in the late Callovian and Oxfordian. The oyster and Gryphaea data show a similar pattern warming followed by cooling. Oxygen isotope thermometry based on shark tooth enamel (Dromart et al. 2003) has also been interpreted to indicate a severe cooling at the Middle-Late Jurassic transition. In the studies of Dromart et al. (2003) and Dera et al. (2011) seawater cooling is inferred to have begun in the Middle or Late Callovian. Notably our study suggests that the cooling (of up to 5 degrees) occurs within the Late Callovian (Athleta) and Early Oxfordian (Mariae) zones, after the positive carbon isotope excursion.

Late Jurassic (Callovian-Kimmeridgian) clumped isotope thermometry (Wierzbowski et al. 2018; Vickers et al. 2020, 2021) show near constant seawater temperatures across this interval, despite an accompanying shift to more negative $\delta^{18}O_{belemnite}$ values across the same interval. Rather than an increase in temperatures, the decrease in belemnite $\delta^{18}O$ values are interpreted as a decrease in the isotopic composition of seawater as a result of a reduced salinity and freshening (Wierzbowski et al. 2018). So, a decrease in $\delta^{18}O_{seawater}$ may account for some of the Oxfordian – Kimmeridgian warming observed in this study (Figs. 7, 8). A large decline of ~8 PSU is implied. There is unfortunately insufficient clumped isotope data to constrain temperatures across the Middle-Late Jurassic transition.

Palaeobiographical studies of ammonites by Dromart et al., (2003), suggests that in the Late Callovian, there was a southward excursion of Boreal Sea ammonites into warmer waters e.g., Kosmoceratidae readily populated Southern Europe (Lamberti Zone, Portugal). This migration of ammonite fauna into warmer waters, suggests a decline in sea surface temperatures during the Late Callovian. Furthermore, sequence stratigraphy studies have suggested there was a transgression peaking in the Middle Callovian – correlating with warmest temperatures, and a sea level low stand and regressive event in the Late Callovian–Early Oxfordian (e.g., turbidites in

Atlantic, the North Sea, Oman and Algeria) (Dromart et al., 2003) followed by mid-Oxfordian maximum flooding (Husinec et al., 2022).

A correlation with the demise of carbonate production rates in the oceans during at the Callovian – Oxfordian boundary (Donnadieu et al., 2011), could have increased seawater alkalinity and caused a reduction in atmospheric CO_2, therefore generating a short-term cooling period (Wierzbowski et al., 2013). Therefore, the positive $\delta^{13}C$ excursion, followed by a positive $\delta^{18}O$ shift peaking in the Late Callovian and continuing into the early Oxfordian, as noted above could be associated with enhanced carbon burial and cooling induced by carbon drawdown (e.g., Dromart et al., 2003; Nunn and Price, 2010; Pellenard et al., 2014). Even allowing for some polar amplification, whether the cooling at ~40°N was sufficient to see ice sheet formation (Dromart et al., 2003; Pellenard et al., 2014) is questionable. For example, biogenic carbonate oxygen isotope records from the Russian Platform, suggest that the southward ammonite fauna migrations in the Callovian and Oxfordian and the presence of colder bottom waters, is the actually a result of changes in marine current circulation due to the opening and closing of basins related to high/low stands during the Callovian and Oxfordian (Wierzbowski et al., 2013).

6. Conclusions

The belemnite, oyster and Gryphaea samples provide the first stratigraphic analysis of $\delta^{18}O$ and $\delta^{13}C$ isotope data at the Middle –Late Jurassic transition in Southern England, offer valuable evidence regarding the prevailing palaeoclimatic conditions. Most samples are well-preserved. Integration the results from this study with published $\delta^{18}O$ and $\delta^{13}C$ datasets, shows a negative shift in $\delta^{18}O$, indicating a temperature rise (Bajocian-Middle Callovian) followed by more positive $\delta^{18}O$ values (a cooling of up to 5 degrees) occurring within the Late Callovian (Athleta) and Early Oxfordian (Mariae) zones. This cooling agrees with earlier suggestions of a cooling episode at the

Middle –Late Jurassic transition, although such trends are less apparent in larger datasets (e.g., Dera et al. 2011). This cooling occurs after a prominent the positive carbon isotope excursion, possibly associated with enhanced organic carbon burial. A large positive carbon isotope excursion in the middle Callovian and remaining positive until the middle Oxfordian has also been observed by Bartolini et al. (1999), Katz et al. (2005) and Nunn et al. (2009) revealing a consistency in isotopic trends. Whether there was continental ice formation during this cooling episode is still debated (Wierzbowski and Rogov, 2011; Donnadieu et al. 2011). A cooling of 3-5 degrees at mid latitudes does not necessarily point to polar ice formation. If Jurassic polar climates were truly warm (e.g., Jenkyns et al., 2012; Vickers et al., 2019) such a degree of cooling would undoubtedly lead to cooler polar temperatures – but only with seasonal ice (e.g., Sellwood and Valdes, 2008).

Acknowledgements

We are grateful for the technical support provided by staff at the University of Plymouth. BH study visit to Plymouth, UK was supported by the Erasmus programme and the NRCFH (OTKA) project K135309.

References

Alberti, M., Fürsich, F.T., Pandey, D.K., Ramkumar, M. 2012. Stable isotope analyses of belemnites from the Kachchh Basin, western India: paleoclimatic implications for the Middle to Late Jurassic transition. Facies, 58, 261–278.

Anderson, T.F., Arthur, M.A., 1983. Stable isotopes of oxygen and carbon and their application to sedimentologic and environmental problems. In: Arthur, M.A., Anderson, T.F., Kaplan, I.R., Veizer, J., Land, L.S. (Eds.), Stable Isotopes in Sedimentary Geology: Society of Economic Paleontologists and Minerologists, Short Course Notes, 10, 1–151.

Anderson, T.F., Popp, B.N., Williams, A.C., Ho, L.Z., Hudson, J.D., 1994. The stable isotopic records of fossils from the Peterborough Member, Oxford Clay Formation (Jurassic), UK: paleoenvironmental implications. J. Geol. Soc. Lond., 151, 125–138.

Arkell, W.J. 1947. The Geology of the Country around Weymouth, Swanage, Corfe and Lulworth. Memoir of the Geological Survey, 386 pp.

Banker, R.M.W., Sumner, D.Y., 2020 Structure and distribution of chalky deposits in the Pacific oyster using x-ray computed tomography (CT). Scientific Reports, 10:12118

Barskov, I.S. Kiyashko 2000 Thermal regime variations in the Jurassic marine basin of the East European Platform at the Callovian–Oxfordian boundary: evidence from stable isotopes in belemnite rostra. Doklady Earth Sciences.

Bartolini, A., Baumgartner, P.O. & Guex, J. 1999. Middle and Late Jurassic radiolarian palaeoecology versus carbon-isotope stratigraphy. Palaeogeography, Palaeoclimatology, Palaeoecology, 145, 43–60.

Brand U., Veizer, J 1980 Chemical Diagenesis of a Multicomponent Carbonate System--1: Trace Elements. Jour. of Sediment. Petrol. 50, 1219–1236.

Callomon, J.H., Cope J.C.W. 1995. The Jurassic geology of Dorset. In Taylor, P. D (ed.), 1995. Field Geology of the British Jurassic. Geological Society, London

Carrigan, W.J., Cole, G., Colling, E.L., Jones, P.J., 1995. Geochemistry of the Upper Jurassic Tuwaiq Mountain and Hanifa Formation Petroleum Source Rocks of Eastern Saudi Arabia. Petroleum Source Rocks, p. 67– 87.

Cope, J.C.W., 2016. Geology of the Dorset coast. Geologists’ Association Guide No. 22. London: The Geologists’ Association. 2nd Edition.

Dera, G., Brigaud, B., Monna, F., Laffont, R., Pucéat, E., Deconinck, J.-F., Pellenard, P., Joachimski, M.M. and Durlet, C. 2011. Climatic ups and downs in a disturbed Jurassic world. Geology, 39, 215–218.

Ditchfield, P.W., 1997. High northern palaeoaltitude Jurassic-Cretaceous palaeotemperature variation: new data from Kong Karls Land, Svalbard. Palaeogeography, Palaeoclimatology, Palaeoecology, 130, 163–175.

Donnadieu, Y., Dromart, G., Goddéris, Y., Pucéat, E., Brigaud, B., Dera, G., Dumas, C., Olivier, N. 2011. A mechanism for brief glacial episodes in the Mesozoic greenhouse. Paleoceanography, 26, PA3212.

Dromart, G., Garcia, J. P., Picard, S., Atrops, F., Lécuyer, C. and Sheppard, S.M.F. 2003. Ice age at the Middle–Late Jurassic transition? Earth and Planetary Science Letters, 213, 205–220.

Gradstein, F.M., Ogg, J.G., Schmitz, M.D. and Ogg, G.M. 2020. Geologic time scale 2020. Amsterdam: Elsevier. 978–979.

Gröcke, D., Price, G.D., Ruffell, A., Mutterlose, J., Baraboshkin, E., 2003. Isotopic evidence for Late Jurassic-Early Cretaceous climate change. Palaeogeography, Palaeoclimatology, Palaeoecology, 202, 272–283.

Hendry, J.P., Kalin, R., 1997. Are oxygen and carbon isotopes of mollusc shells reliable palaeosalinity indicators in marginal marine environments? A case study from the Middle Jurassic of England. Journal of the Geological Society 154, 321–333.

House, M.R., 1993 Geology of the Dorset Coast 2nd Edition (1993) Geologists Association Guide

Hudson, J.D. and Martill, D.M., 1991. Fossils of the Oxford Clay. Palaeontological Association Field Guide to Fossils, 4, 286 pp.

Husinec, A., Read, J.F., Prtoljan B., 2022. Middle and Late Jurassic record of sea-level, sequence development, and carbon-isotope fluctuations, Tethyan Adriatic Carbonate Platform, Croatia. Palaeogeography, Palaeoclimatology, Palaeoecology, 599, 1 111030.

Jenkyns, H.C. 1996. Relative sea-level change and carbon isotopes: data from the Upper Jurassic (Oxfordian) of central and southern Europe. Terra Nova, 8, 75–85.

Jenkyns, H.C., Jones, C.E., Gröcke, D.R., Hesselbo, S.P. and Parkinson, D.N. 2002. Chemostratigraphy of the Jurassic System: applications, limitations and implications for palaeoceanography. Journal of the Geological Society, 159, 351–378.

Jenkyns, H.C., Schouten-Huibers, L., Schouten, S., Sinninghe Damsté, J. 2012. Warm Middle Jurassic-Early Cretaceous high-latitude sea-surface temperatures from the Southern Ocean. Clim. Past 8

Katz, M.E., Wright J.D., Miller, K.G., Cramer, B.S., Fennel, K., Falkowski, P.G. 2005 Biological overprint of the geological carbon cycle. Marine Geology, 217, 323–338.

Kele, S., Breitenbach, S.F.M., Capezzuoli, E., Meckler A.N., Ziegler, M., Millan, I.M., Kluge, T., Deák, J., Hanselmann, K., John, C.M., Yan H., Liu, Z., Bernasconi, S.M., 2015. Temperature dependence of oxygen-and clumped isotope fractionation in carbonates: a study of travertines and tufas in the 6–95C temperature range. Geochim. Cosmochim. Acta. 168, 172–192.

Kenig, F., Hayes, J.M., Popp, B.N., Summons, R.E. 1994 Isotopic biogeochemistry of the Oxford Clay Formation (Jurassic), UK. Journal of the Geological Society, London, 151, 139–152.

Krenker, -N., Lindström, S., Bodin S. 2019. A major sea-level drop briefly precedes the Toarcian oceanic anoxic event: implication for Early Jurassic climate and carbon cycle. Scientific Reports 9, Article number: 12518.

Lécuyer, C., Picard, S., Garcia, J.-P., Sheppard, S.M.F., Grandjean, P., Dromart, G., 2003. Thermal evolution of Tethyan surface during the Middle–Late Jurassic: evidence from 18O values of marine fish teeth. Paleoceanography 18. doi:10.1029/2002PA000863

Li, Q., McArthur J., Doyle, P., Janssen, N., Leng, M.J., Müller, W., Reboulet, S., 2013. Evaluating Mg/Ca in belemnite calcite as a palaeo-proxy. Palaeogeography, Palaeoclimatology, Palaeoecology, 388, 98–108.

Louis-Schmid, B., Rais, P., Bernasconi, S.M., Pellenard, P., Collin, P.-Y., Weissert, H. 2007. Detailed record of the mid-Oxfordian (Late Jurassic) positive carbon-isotope excursion in two hemipelagic sections (France and Switzerland): A plate tectonic trigger? Palaeogeography, Palaeoclimatology, Palaeoecology, 248, 459–472.

McArthur, J.M., Doyle, P., Leng, M.J., Reeves, K., Williams, C.T., Garcia-Sanchez, R., Howarth, R.J. 2007. Testing palaeo-environmental proxies in Jurassic belemnites: Mg/Ca, Sr/Ca, Na/Ca, δ18O and δ13C. Palaeogeography, Palaeoclimatology, Palaeoecology, 252, 464–480.

Malchus, N., Aberhan, M., 1998. Transitional Gryphaeate/Exogyrate Oysters (Bivalvia: Gryphaeidae) from the Lower Jurassic of Northern Chile. Journal of Paleontology, 72, 619–663.

Martin-Garin B., Lathuiliere B., Geister, J., Ramseyer, K., 2010 Oxygen isotopes and climatic control of Oxfordian coral reefs (Jurassic, Tethys). Palaios, 25, 721–729.

Mettam, C., Johnson, A.L.A., Nunn E.V., Schöne, B.R., 2014. Stable isotope ($\delta^{18}O$ and $\delta^{13}C$) sclerochronology of Callovian (Middle Jurassic) bivalves (*Gryphaea (Bilobissa) dilobotes*) and belemnites (*Cylindroteuthis puzosiana*) from the Peterborough Member of the Oxford Clay Formation (Cambridgeshire, England): Evidence of palaeoclimate, water depth and belemnite behaviour. Palaeogeography, Palaeoclimatology, Palaeoecology, 399, 187–201.

Milliman, J.D. 1974. Marine Carbonates. Springer-Verlag, New York .

Nordt, L., Breecker, D., , J. 2021 Jurassic greenhouse ice-sheet fluctuations sensitive to atmospheric CO2 dynamics, Nature Geoscience

Nunn, E. V., Price, G. D., 2010. Late Jurassic (Kimmeridgian–Tithonian) stable isotopes ($\delta^{18}O$, $\delta^{13}C$) and Mg/Ca ratios: New palaeoclimate data from Helmsdale, north east Scotland. Palaeogeography, Palaeoclimatology, Palaeoecology. 292, 325–335.

Nunn E.V., Price G.D., Hart M.B., Page K.N., Leng M.J., 2009. Isotopic signals from Callovian - Kimmeridgian (Middle Upper Jurassic) belemnites and bulk organic carbon, Staffin Bay, Isle of Skye, Scotland. Journal of the Geological Society, 166, 633–664.

Padden, H., Weissert, H., De Rafelis, M., 2001. Evidence for Late Jurassic release of methane from gas hydrate. Geology 29, 223–226.

Palmer, T.J., Wilson, M.A. 1990. Growth of ferruginous oncoliths in the Bajocian (Middle Jurassic) of Europe. Terra Nova 2, 142-147.

Page, K.N., 1989. A stratigraphical revision for the English Lower Callovian. Proceedings of the Geologists Association, 100, 363–382.

Pearce C.R., Hesselbo, S.P., Coe, A.L. 2005. The mid-Oxfordian (Late Jurassic) positive carbon-isotope excursion recognised from fossil wood in the British Isles. Palaeogeography, Palaeoclimatology, Palaeoecology, 221, 343–357.

Pellenard, P., Tramoy, R., Pucéat, E., Huret, E., Martinez, M., Bruneau, L., Thierry, J. 2014. Carbon cycle and seawater palaeotemperature evolution at the Middle–Late Jurassic transition, eastern Paris Basin (France). Marine and Petroleum Geology, 53, 30–43.

Price, G.D. 2010. Carbon-isotope stratigraphy and temperature change during the Early–Middle Jurassic (Toarcian–Aalenian), Raasay, Scotland, UK. Palaeogeography, Palaeoclimatology, Palaeoecology, 285, 255–263.

Price, G.D., Page, K.N., 2008. A carbon and oxygen isotopic analysis of molluscan faunas from the Callovian-Oxfordian boundary at Redcliff Point, Weymouth, Dorset: implications for belemnite behaviour. Proceedings of the Geologists' Association, 119, 153–160.

Price, G. D., Rogov, M., 2009. An isotopic appraisal of the Late Jurassic greenhouse phase in the Russian Platform. Palaeogeography, Palaeoclimatology, Palaeoecology, 273, 41–49.

Price, G.D., Teece, C. 2010. Reconstruction of Jurassic (Bathonian) palaeosalinity using stable isotopes and faunal associations. J. Geol. Soc. London, 167, 1199–1208.

Price, G.D., Janssen, N.M.M., Martinez, M., Company, M., Vandevelde, J.H., Grimes, S.T. 2018. A High-Resolution Belemnite Geochemical Analysis of Early Cretaceous (Valanginian-Hauterivian) Environmental and Climatic Perturbations. Geochemistry, Geophysics, Geosystems, 19, 3832–3843.

Price, G.D., Wilkinson, D., Hart, M.B., Page, K.N., Grimes, S.T. 2009. Isotopic analysis of coexisting Late Jurassic fish otoliths and molluscs: Implications for upper-ocean water temperature estimates. Geology, 37, 215–218.

Price, G.D., Hart, M.B., Wilby, P.R., Page, K.N., 2015. Isotopic analysis of Jurassic (Callovian) mollusks from the Christian Malford Lagerstätte (UK): implications for ocean water temperature estimates based on belemnoids. Palaios, 30, 645–654.

Rosales, I., Quesada, S., Robles, S., 2001 Primary and diagenetic isotopic signals in fossils and hemipelagic carbonates: the Lower Jurassic of northern Spain. Sedimentology, 48, 1149–1169.

Ruebsam, W., Al-Husseini, M.I., 2021. Orbitally synchronized late Pliensbachian–early Toarcian glacio-eustatic and carbon-isotope cycles. Palaeogeography, Palaeoclimatology, Palaeoecology, 577

Scotese, C.R., 2014. Atlas of Jurassic Paleogeographic Maps, PALEOMAP Atlas for ArcGIS, volume 4, The Jurassic and Triassic, Maps 32-42, Mollweide Projection, PALEOMAP Project, Evanston, IL.

Sellwood, B.W., Valdes, P., 2008. Jurassic climates. Proceedings of the Geologists' Association 119, 5– 17.

Vickers, M.L., Bajnai, D., Price, G.D., Linckens, J., Fiebig, J. 2019. Southern high-latitude warmth during the Jurassic–Cretaceous: New evidence from clumped isotope thermometry. Geology 47, 724–728.

Vickers, M.L., Fernandez, A., Hesselbo, S.P., Price, G.D., Bernasconi, S.M., Lode, S., Ullmann, C.V., Thibault, N., Hougård, I.W., and Korte, C., 2020, Unravelling Middle to Late Jurassic palaeoceanographic and palaeoclimatic signals in the Hebrides Basin using belemnite clumped isotope thermometry: Earth and Planetary Science Letters, 546, 116401.

Vickers, M.L., Bernasconi, S.M., Ullmann, C.V., Lode, S., Looser, N., Morales, L.G., Price, G.D., Wilby, P.R., Hougård, I.W., Hesselbo, S.P. & Korte, C., 2021. Marine temperatures underestimated for past greenhouse climate. Sci Rep 11, 19109.

Weissert, H. 1989. C-isotope stratigraphy, a monitor of paleoenvironmental change: a case study from the early Cretaceous. Surveys in Geophysics 10, 1–61.

Wierzbowski, H., 2004. Carbon and oxygen isotope composition of Oxfordian – Early Kimmeridgian belemnite rostra: palaeoenvironmental implications for Late Jurassic seas. Palaeogeography, Palaeoclimatology, Palaeoecology, 203, 153–168.

Wierzbowski, H., Joachimski, M., 2007. Reconstruction of late Bajocian-Bathonian marine palaeoenvironments using carbon and oxygen isotope ratios of calcareous fossils from the Polish Jura Chain (central Poland). Palaeogeography, Palaeoclimatology, Palaeoecology, 254, 523–540.

Wierzbowski, H., Błażejowski, B., Tyborowski, D. 2019. Oxygen Isotope profiles of uppermost Jurassic vertebrate teeth and oyster shells: A record of paleoenvironmental changes and animal habitats. Palaios, 34, 585–599.

Wierzbowski, H., Dembicz, K., Praszkier, T., 2009. Oxygen and carbon isotope composition of Callovian-Lower Oxfordian (Middle-Upper Jurassic) belemnite rostra from central Poland: A record of a Late Callovian global sea-level rise? Palaeogeography, Palaeoclimatology, Palaeoecology, 283, 182–194.

Wierzbowski, H., Rogov, M., 2011. Reconstructing the palaeoenvironment of the Middle Russian Sea during the Middle–Late Jurassic transition using stable isotope ratios of cephalopod shells and variations in faunal assemblages. Palaeogeography, Palaeoclimatology, Palaeoecology, 299, 250–264.

Wierzbowski, H., Rogov, M.A., Matyja, B.A., Kiselev, D. and Ippolitov, A. 2013. Middle–Upper Jurassic (Upper Callovian–Lower Kimmeridgian) stable isotope and elemental records of the Russian Platform: Indices of oceanographic and climatic changes. Global and Planetary Change, 7, 196–212.

Wierzbowski, H., Bajnai, D., Wacker, U., Rogov, M.A., Fiebig, J., Tesakova, E.M., 2018. Clumped isotope record of salinity variations in the Subboreal Province at the Middle–Late Jurassic transition. ScienceDirect Global and Planetary Change 167, 172–189.

Wright, J.K. 1986 A new look at the stratigraphy, sedimentology and ammonite fauna of the Corallian Group (Oxfordian) of South Dorset. Proceedings of the Geologists' Association, 97, 1–21.

Wright, J.K. 2014. A new section through the Corallian Group (Oxfordian, Upper Jurassic) rocks of Calne, Wiltshire, Southern England. Proceedings of the Geologists’ Association, 125, 83–95.

Wright, J.K., 2016. The stratigraphy and geological setting of the Oxfordian Corallian Group around Steeple Ashton and Westbury, Wiltshire, U.K. Proceedings of the Geologists’ Association, 127, 266–279.

Wright, J.K. and Cox, B.M., 2001. British Upper Jurassic Stratigraphy (Oxfordian to Kimmeridgian). Geological Conservation Review 21. Joint Nature Conservation Committee, Peterborough, 266.

Zhou, J., Poulsen, C.J., Pollard, D., White, T.S., 2008. Simulation of modern and middle Cretaceous marine $\delta^{18}O$ with an ocean–atmosphere general circulation model. Paleoceanography 23, PA3223.

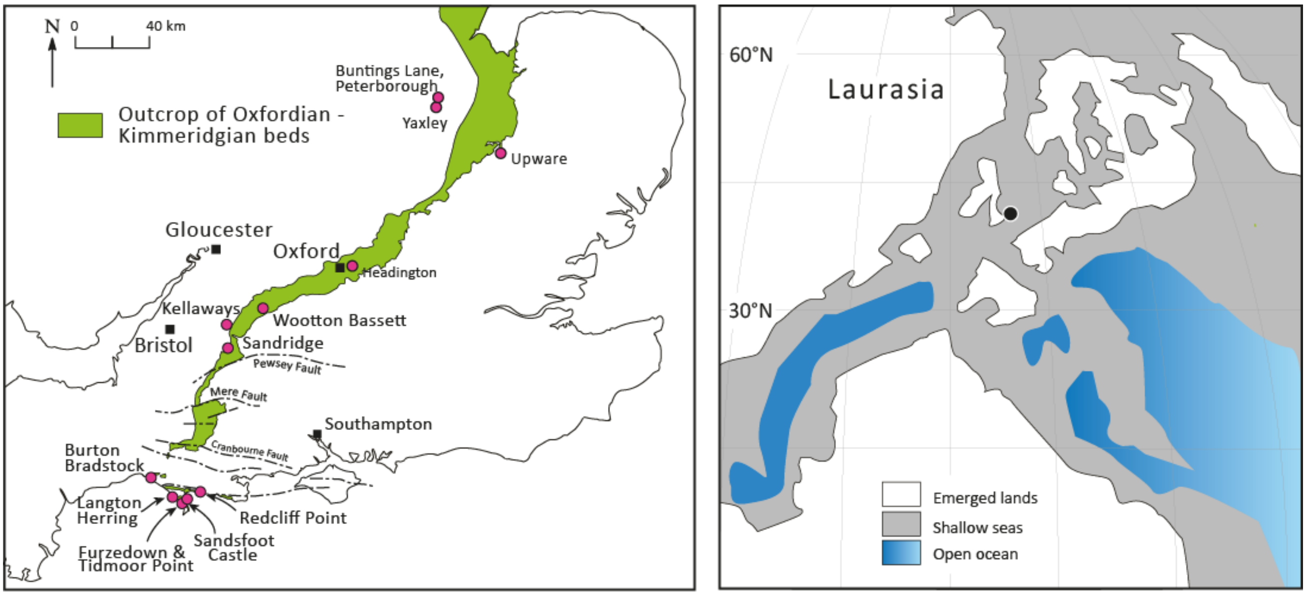

Figure 1 Outcrop map for the Lias Group in England and Wales and showing the location of Dorset, UK (after Wright and Cox, 2001). Late Jurassic (Oxfordian) palaeogeographic map modified from Scotese (2014).

Figure 2. Sampling locations across Dorset and Wiltshire illustrating the variable nature of exposures. A. Well exposed Inferior Oolite in a large fallen block at Burton Cliff, Burton

Bradstock, Dorset. B. Oxford Clay exposed in low cliff exposures at Tidmoor Point, Fleet Lagoon, Dorset, C Fallen blocks of the Sandsfoot Grit Member Sandsfoot Castle, Weymouth, Dorset. D. The type locality of the Kellaways Formation, River Avon, west of Tytherton, Wiltshire, and E. Cliff exposure of the Callovian-Oxfordian boundary succession (Weymouth Member) at Redcliff Point near Weymouth, Dorset, UK.

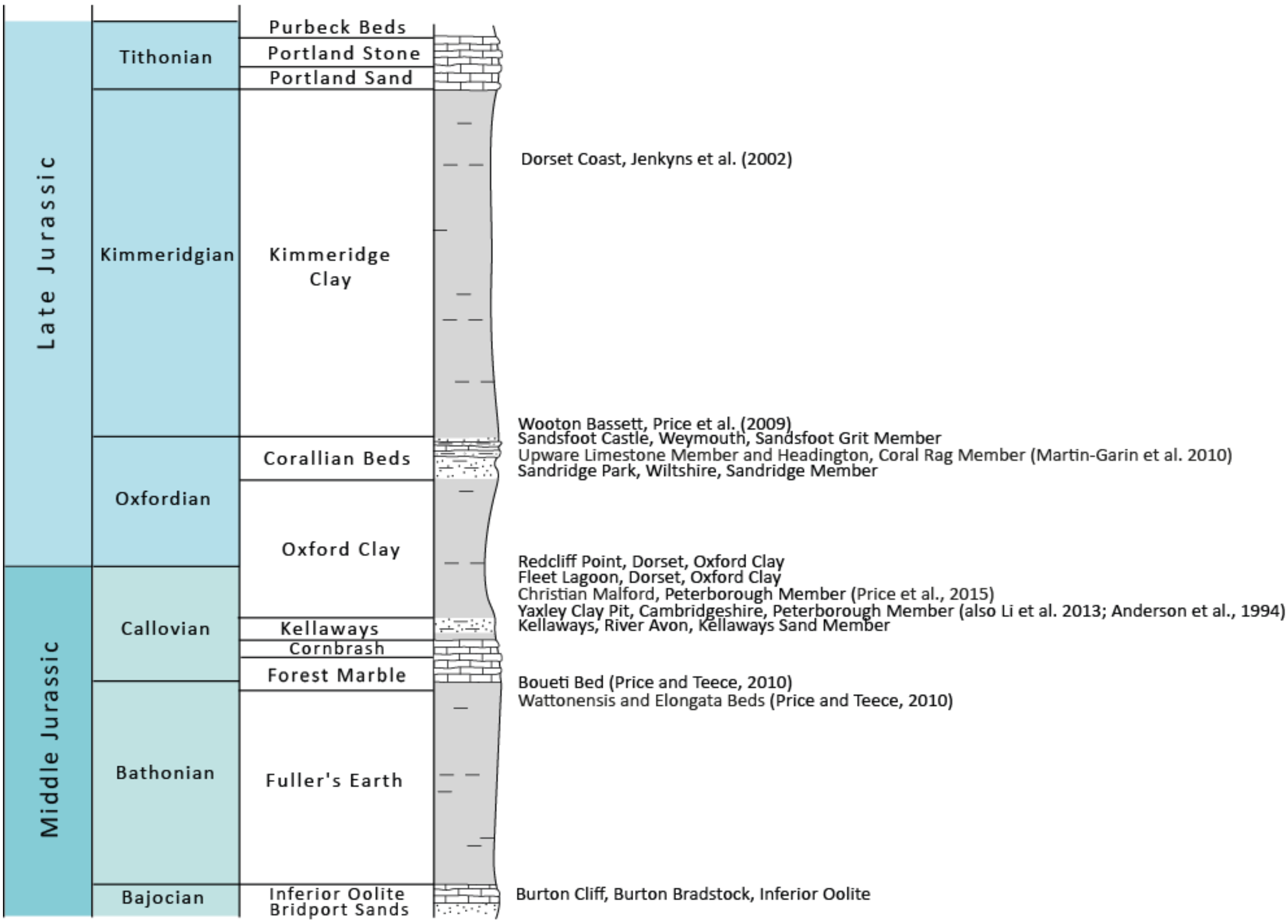

Figure 3. A summary of the Middle and Upper Jurassic stratigraphic succession of Dorset area (modified from Wright, 1986; House 1993) with sampling (location) levels and published sources of data.

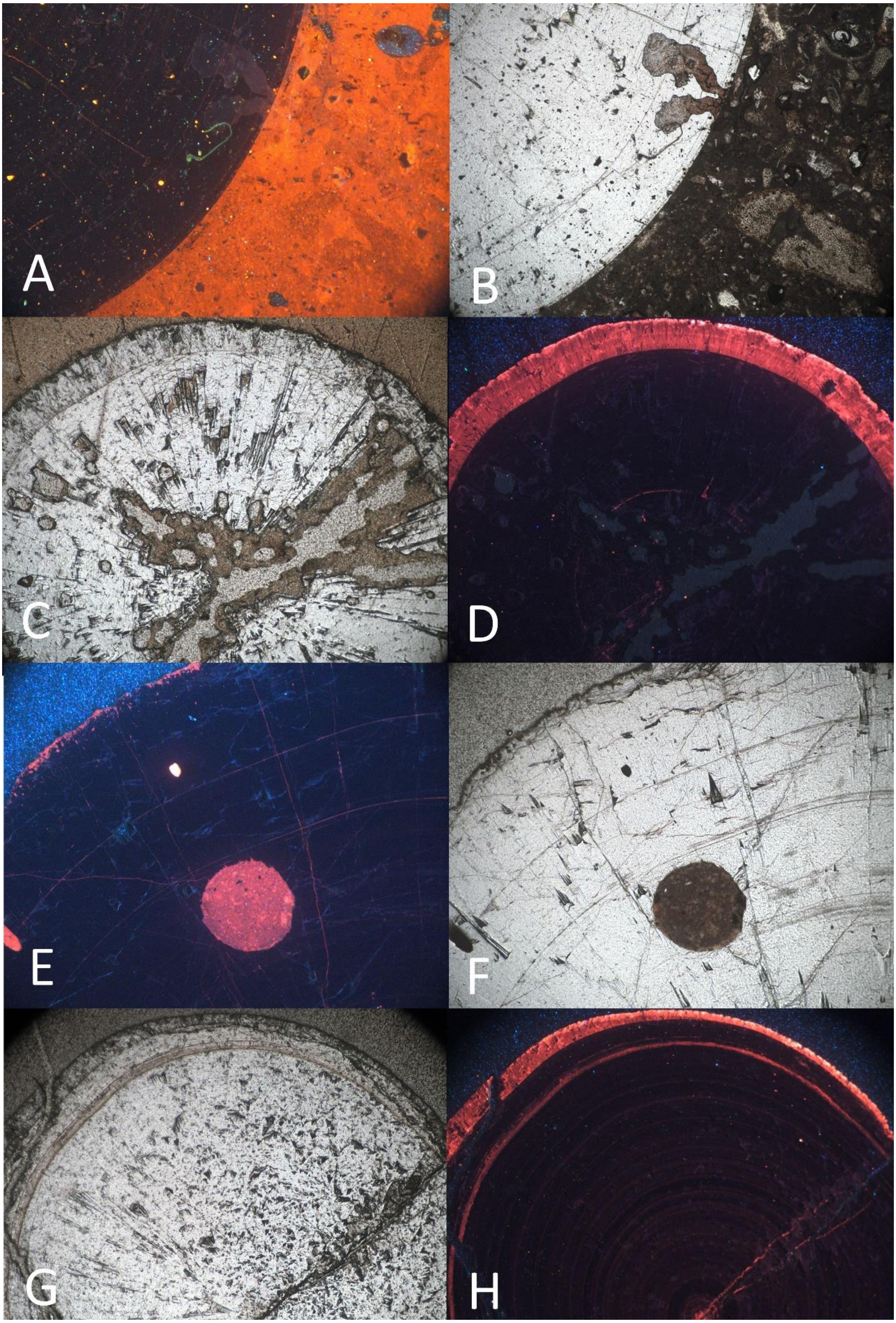
A
B
C
D
E
F
G
H

Figure 4 CL and plane polarised light photomicrographs (A, B) of non-luminescent rostrum within highly luminescent carbonate (sample BBRC1); plane polarised light and CL photomicrographs (C, D) non-luminescent rostrum with luminescent margin (Sample TPB2); (E, F) non-luminescent rostrum with luminescent sediment infilled boring (Sample BBSB1) and plane polarised light and CL photomicrographs (G, H) luminescent apical line area of rostrum, fracture and luminescent margin (Sample FDB12).

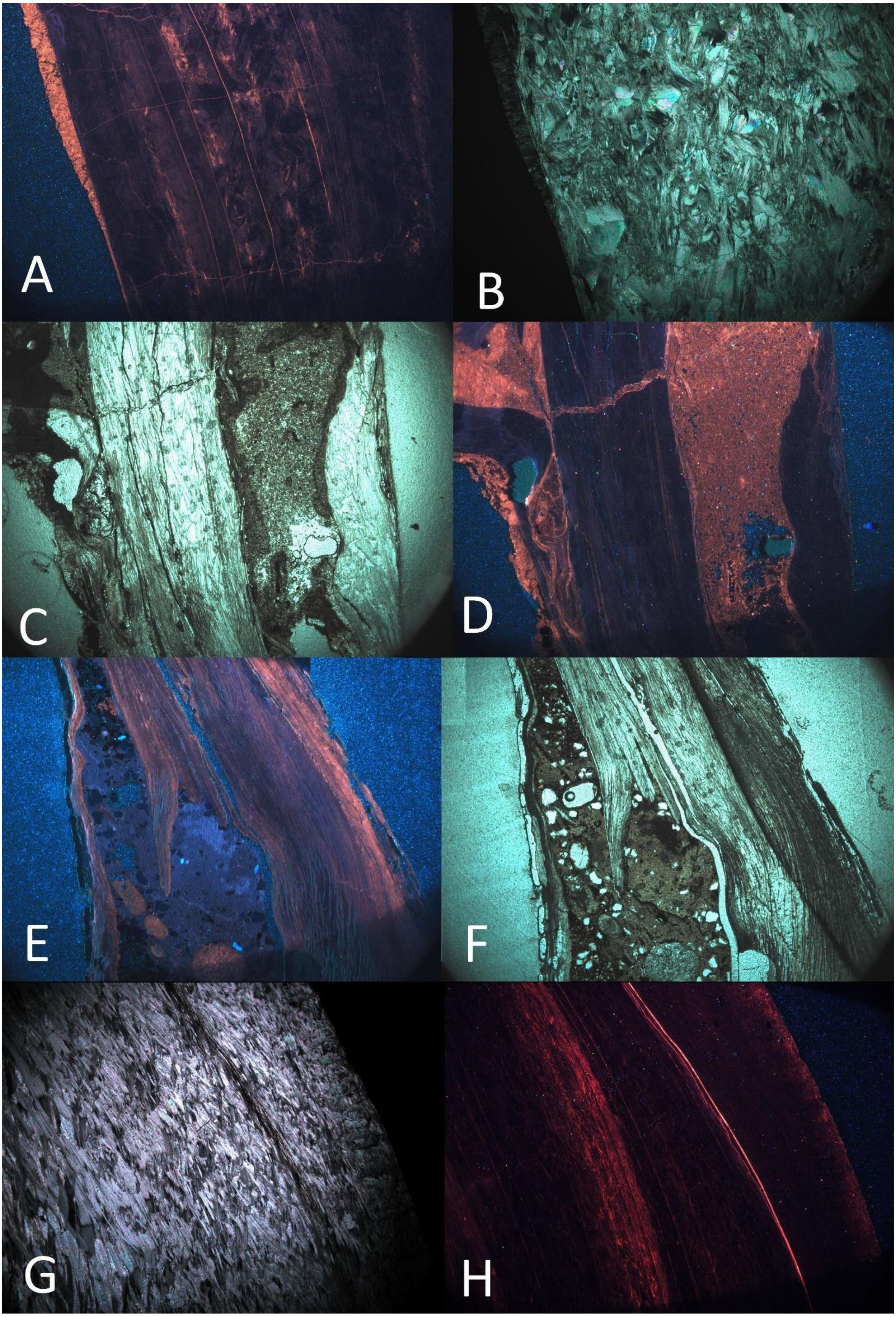
A
B
C
D
E
F
G
H

Figure 5. CL and crossed polarised light photomicrographs (A, B) of Gryphaea showing complex cross foliation, largely non-luminescent and thin luminescent fractures (sample FDG7); plane polarised light and CL photomicrographs (C, D) of non-luminescent oyster with strongly luminescent sediment and cement within interspersed chambers and luminescent sparry calcite fracture (sample TPO4); CL and plane polarised light photomicrographs (E, F) showing well-preserved largely non- luminescent foliated shells, with luminescent calcite along the outer shell margin, and sediment infilled interspersed lens shaped chambers (Sample SCO14) and crossed polarised light and CL photomicrographs (G, H) of Gryphaea showing complex cross foliation, largely non-luminescent and thin luminescent fractures (sample TPG6).

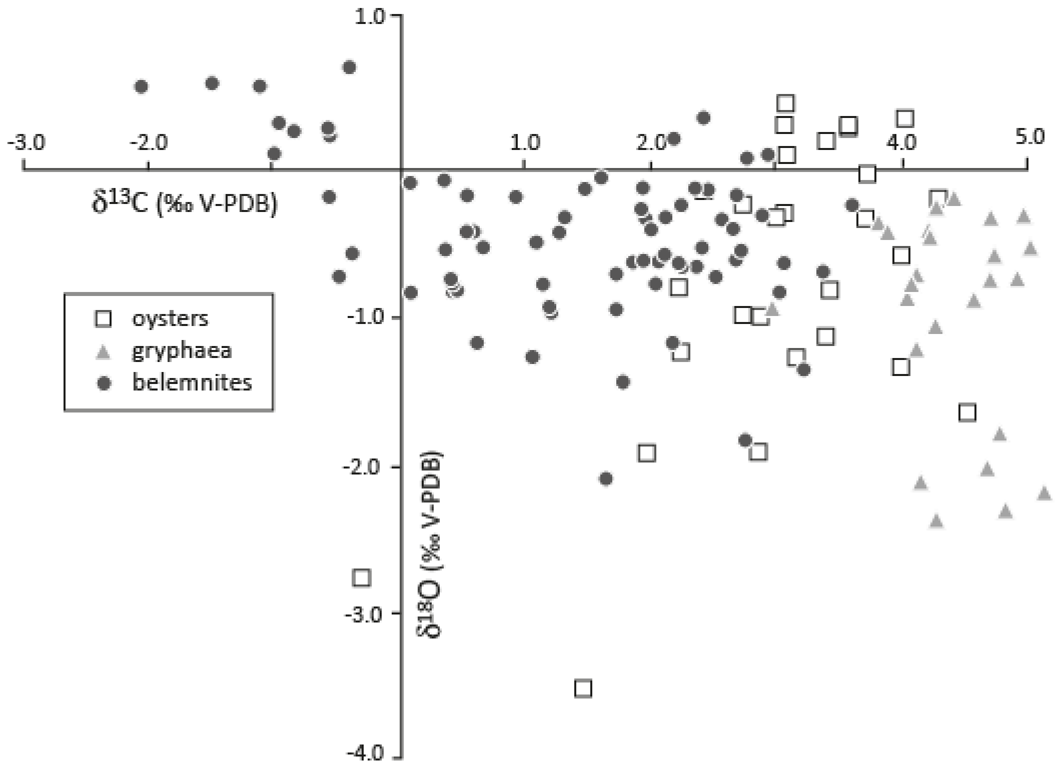

Figure 6. Cross plot of $\delta^{18}O$ and $\delta^{13}C$ data from the belemnite specimens, Gryphaea and oysters

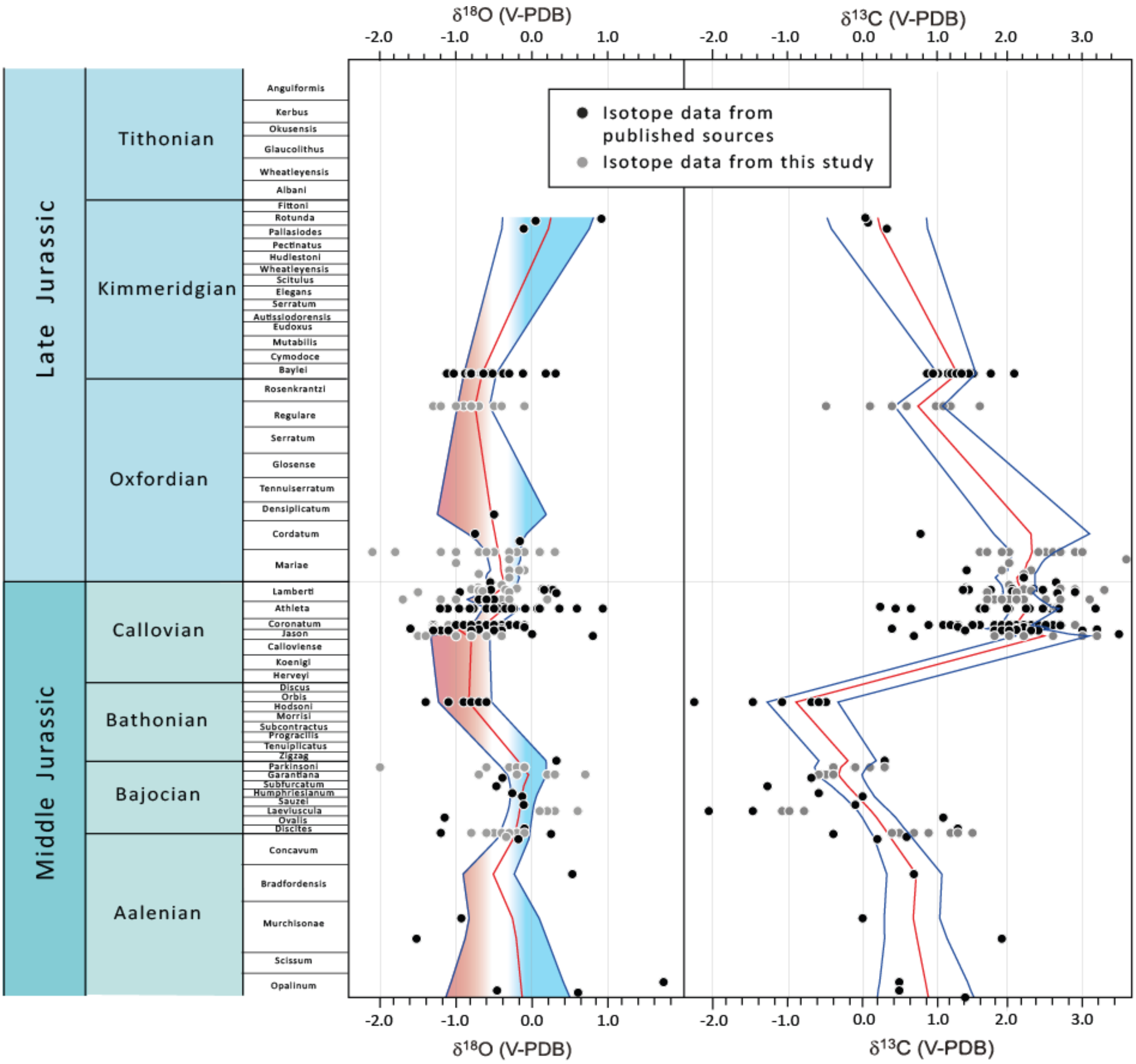

Figure 7 Belemnite $\delta^{18}O$ and $\delta^{13}C$ trends and LOESS curve fitting. Data are scaled to the GTS2020 timescale, based on ammonite zonation (from Wright and Cox 2001; House, 1993). The $\delta^{18}O$ curve has been coloured red to blue to indicate that more negative $\delta^{18}O$ may reflect warmer conditions, and more positive values with cooler conditions. Data presented is from this study and published sources noted in the text.

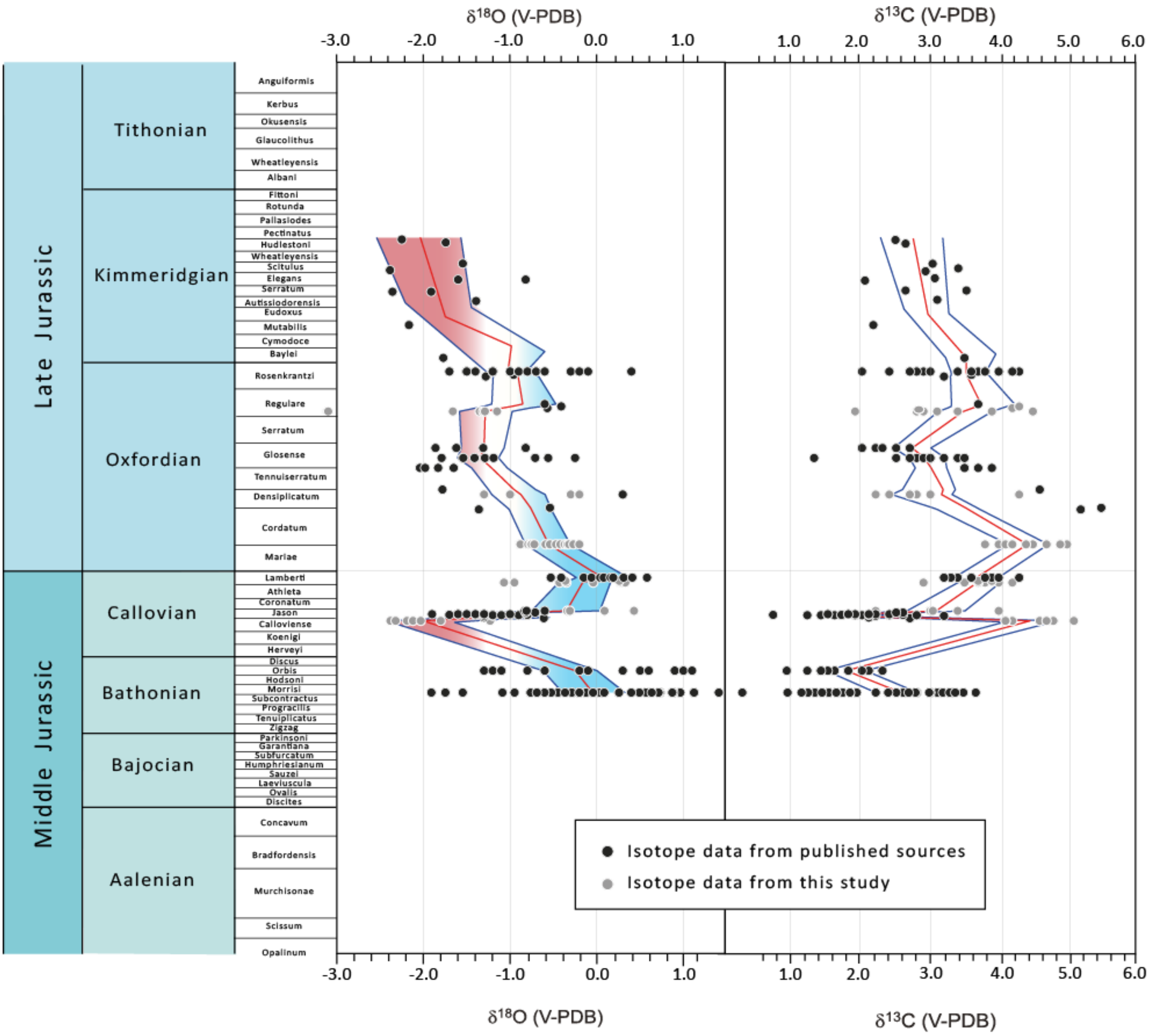

Figure 8. Oyster and Gryphaea $\delta^{18}O$ and $\delta^{13}C$ values trends and LOESS curve fitting. Data are scaled to the GTS2020 timescale, based on ammonite zonation (from Wright and Cox 2001; House, 1993). The $\delta^{18}O$ curve has been coloured red to blue to indicate that more negative $\delta^{18}O$ may reflect warmer conditions, and more positive values with cooler conditions. Data presented is from this study and published sources noted in the text.